Environmental Science
Water Research & Technology

ROYAL SOCIETY OF CHEMISTRY

PAPER

View Article Online
View Journal | View Issue

Cite this: *Environ. Sci.: Water Res. Technol.*, 2024, **10**, 1245

Removal of phosphorus and fluorine from wastewater containing PF_6^- *via* accelerated decomposition by Al^{3+} and chemical precipitation for hydrometallurgical recycling of lithium-ion batteries†

Takuto Miyashita, * Kouji Yasuda * and Tetsuya Uda *

During hydrometallurgical recycling of lithium-ion batteries (LIBs), one important challenge is the efficient treatment of wastewater containing $LiPF_6$ used as a lithium salt in the LIBs. The difficulty of the treatment is attributed to the persistence of PF_6^- in aqueous solutions. In this study, the accelerated decomposition of PF_6^- by Al^{3+} at an elevated temperature and the removal of phosphorus and fluorine by chemical precipitation were attempted. These reactions were analyzed using a pH electrode and fluoride-ion selective electrode, and by a distillation method for total fluorine analysis, ICP-AES, ion chromatography, XRD, and WDS. The results showed that when 10 mM $LiPF_6$ aqueous solution containing 100 mM $Al_2(SO_4)_3$ was kept at 90 °C for 24 h, more than 90% of the PF_6^- was decomposed into PO_4^{3-} and F^-. The produced PO_4^{3-} and F^- were coprecipitated with $Ca_6Al_2(SO_4)_3(OH)_{12}$ (ettringite) by adding sufficient $Ca(OH)_2$. The concentrations of the total phosphorus and total fluorine in the supernatant after precipitation were 0.028 mM and 0.77 mM, respectively. Here, the pH after the decomposition of 10 mM PF_6^- decreases to around 1 due to the formation of H^+ during the decomposition, which may be too low for some practical cases. For this problem, the decomposition of PF_6^- in various pre-mixed solutions of $Al_2(SO_4)_3$ and $Ca(OH)_2$ was also examined. As a result, when the prepared molar ratio was Al/Ca > 2/3, the decomposition of PF_6^- proceeded, and the pH decrease accompanying the decomposition was alleviated due to the buffer effect of the $Al(OH)_3$ precipitate.

Received 22nd November 2023,
Accepted 28th March 2024

DOI: 10.1039/d3ew00854a

rsc.li/es-water

Water impact

The method for faster decomposition of PF_6^-, which is persistent in aqueous water, is required for wastewater treatment. The efficient decomposition of PF_6^- and the removal of phosphorus and fluorine were achieved using $Al_2(SO_4)_3$ and $Ca(OH)_2$. This method is applicable for treating wastewater exhausted in hydrometallurgical recycling of lithium-ion batteries.

1. Introduction

The production of lithium-ion batteries (LIBs) is exponentially increasing year by year towards a decarbonized and sustainable society, which simultaneously leads to the generation of a large number of spent LIBs. In order to recover various valuable elements such as lithium (Li), cobalt (Co), and nickel (Ni) contained in LIBs, efficient recycling methods for spent LIBs are required.[1–3] The recycling processes of spent LIBs currently in commercial use are mainly classified as pyrometallurgical and hydrometallurgical processes.[4–6] In the pyrometallurgical process, spent LIBs are roasted or melted at various temperatures depending on the companies.[7,8] One of the advantages of the pyrometallurgical process is the safe treatment of the flammable organic solvents and active Li remaining in the negative electrode by combustion. On the other hand, the necessity of the treatment of the fluorine-containing gases remains a problem. In addition, Li transfers to the slag under some melting conditions, and the recovery cost of Li could be high. The recycling processes of spent LIBs at room temperature (R.T.) including the hydrometallurgical process are considered as a solution to the problems of the pyrometallurgical process. When recycling of spent LIBs is conducted without roasting, treatment of the fluorine-containing gases is not necessary, and Li remains in the

Department of Materials Science and Engineering, Graduate School of Engineering, Kyoto University, Kyoto, 606-8501, Japan.
E-mail: miyashita.takuto.68s@st.kyoto-u.ac.jp, yasuda.kouji.3v@kyoto-u.ac.jp, uda.tetsuya.5e@kyoto-u.ac.jp

† Electronic supplementary information (ESI) available. See DOI: https://doi.org/10.1039/d3ew00854a

positive electrode or electrolyte. The most important challenge is the safe deactivation of spent LIBs containing flammable organic solvents and active Li that may cause ignition. One of the deactivation methods proposed in the past is comminution in water or an inert atmosphere. The first reported method of comminution of spent LIBs in water at R.T., to the author's knowledge, was a patent by Asaka Riken.[9] Later, other technologies were reported for comminution in water, for example, by Retriev[10] and LiCycle,[11] and for comminution without water under a CO_2 or Ar atmosphere by Recupyl.[12] Our group proposed the submerged comminution in water in an inert atmosphere, especially in lime water (saturated calcium hydroxide ($Ca(OH)_2$) solution), to deactivate the spent LIBs even at a charged state.[13] The submerged comminution in water is superior in terms of low ignition risk to comminution in the gas phase, but treatment of wastewater containing electrolytes of LIBs, *i.e.*, organic solvents such as carbonate ester and Li salts such as $LiPF_6$, is required.[13–15]

Phosphorus (P) and fluorine (F) in aquatic ecosystems cause eutrophication and health hazards, respectively, and effluent standards for wastewater are established in many countries.[16–18] For example, the concentrations of P and F in industrial wastewater are regulated at 16 ppm and 8 ppm, respectively, in the representative Japanese standards. Wastewater containing P is mainly treated by chemical precipitation, crystallization, and biological treatment.[16,17] In the chemical precipitation, P is removed by being coprecipitated with aluminum hydroxide ($Al(OH)_3$) or iron hydroxide ($Fe(OH)_3$) using chlorides or sulfates of aluminum(III) or iron(III). In the crystallization, P is removed as precipitates such as hydroxyapatite ($Ca_5(PO_4)_3(OH)$, reaction (1)) by introducing calcium compounds such as $Ca(OH)_2$.

$$3H_3PO_4 + 5Ca(OH)_2 \rightarrow Ca_5(PO_4)_3(OH) + 9H_2O \quad (1)$$

Wastewater containing F is typically treated by chemical precipitation, crystallization for example by forming calcium fluoride (CaF_2, reaction (2)), membrane treatment, and adsorption methods.[18–20]

$$2HF + Ca(OH)_2 \rightarrow CaF_2 + 2H_2O \quad (2)$$

It is difficult to treat wastewater containing hexafluorophosphate ion (PF_6^-) produced by the ionization of $LiPF_6$ by chemical precipitation or crystallization because PF_6^- is persistent in aqueous solution[21,22] and does not usually form insoluble precipitates with common metal cations as far as we know. The precipitation with non-metallic compounds and the decomposition into PO_4^{3-} and F^- are candidate treatment methods for wastewater containing PF_6^-. As a method of the former, pyridine (C_5H_5N) is reported to form an insoluble precipitate with PF_6^- in reaction (3); to the best of our knowledge, this is the only method that can precipitate with PF_6^- in aqueous solution without decomposition.[23]

$$C_5H_5N + H^+ + PF_6^- \rightarrow C_5H_5NHPF_6 \quad (3)$$

However, the use of pyridine has several problems such as toxicity to humans, flammability, and odorousness. Furthermore, the treatment of pyridine-containing wastewater is costly because combustion or adsorption treatment is required.[24]

On the other hand, some methods to decompose PF_6^- into PO_4^{3-} and F^- were reported according to reaction (4).[22,25]

$$PF_6^- + 4H_2O \rightarrow PO_4^{3-} + 6F^- + 8H^+ \quad (4)$$

One decomposition method patented by some Japanese companies is adding 2–25 wt% hydrochloric acid (HCl) or 35 wt% sulfuric acid (H_2SO_4) into wastewater containing PF_6^- and heating at 50–100 °C for 0.5–5 h.[26–28] In this method, the acid concentration is so strong and the operation temperature is so high that highly corrosion-resistant components are required for the treatment tanks. In addition, the vapor pressure of HF increases under heated acidic conditions,[29] and the treatment of HF-containing gas could be also required. Another decomposition method for PF_6^- is the addition of compounds containing cations working as hard acids such as Zr^{4+}, Th^{4+}, Al^{3+}, and Be^{2+}.[30] The reaction temperatures in the report were only around R.T., and the decomposition rate was not sufficient; for example, the half-lives of PF_6^- in 1.0 mol L^{-1} (M) HCl dissolving 1.0 M Zr^{4+}, 1.5 M Th^{4+}, 2.0 M Al^{3+}, and 1.5 M Be^{2+} were 78 h, 213 h, 767 h, and 1050 h, respectively. The above decomposing methods need improvement in terms of reagent cost and treatment time.

In this study, the accelerated decomposition of PF_6^- by Al^{3+} was attempted at elevated temperature. Chemical precipitation of PO_4^{3-} and F^- produced by the decomposition of PF_6^- was carried out by adding $Ca(OH)_2$. As shown in Fig. 1, two types of procedures were investigated. In procedure A (Fig. 1(a)), $LiPF_6$ solutions containing aluminum sulfate ($Al_2(SO_4)_3$) are heated at 90 °C for 24 h to decompose PF_6^-, followed by adding $Ca(OH)_2$ to remove the produced PO_4^{3-} and F^-. In procedure B (Fig. 1(b)), $LiPF_6$ solutions containing both $Al_2(SO_4)_3$ and $Ca(OH)_2$ at various prepared concentrations are heated at 90 °C for 24 h to determine the best conditions for treating PF_6^-. The supernatants and precipitates of the respective samples are analyzed by various methods. The advantages and disadvantages of procedures A and B are discussed.

2. Methods

2.1. Experimental procedures

Decomposition of PF_6^- in procedure A. In procedure A, a sample solution containing 10 mM $LiPF_6$ and 100 Al mM $Al_2(SO_4)_3$ was prepared by dissolving $LiPF_6$ (Fujifilm Wako Pure Chemical Corporation, 98.0+%) and $Al_2(SO_4)_3{\cdot}14–18H_2O$ (Kanto Chemical Co., Inc., GR) in deionized water (DI, Organo Corporation, Pure Light, <0.1 μS cm^{-1}). As $LiPF_6$ powder reacts readily with moisture in air, it was weighed in a dry Ar glove box and then quickly dissolved in DI water in air. Sample solutions containing 10 mM $LiPF_6$ with various pH levels were prepared by adding a suitable amount of HCl

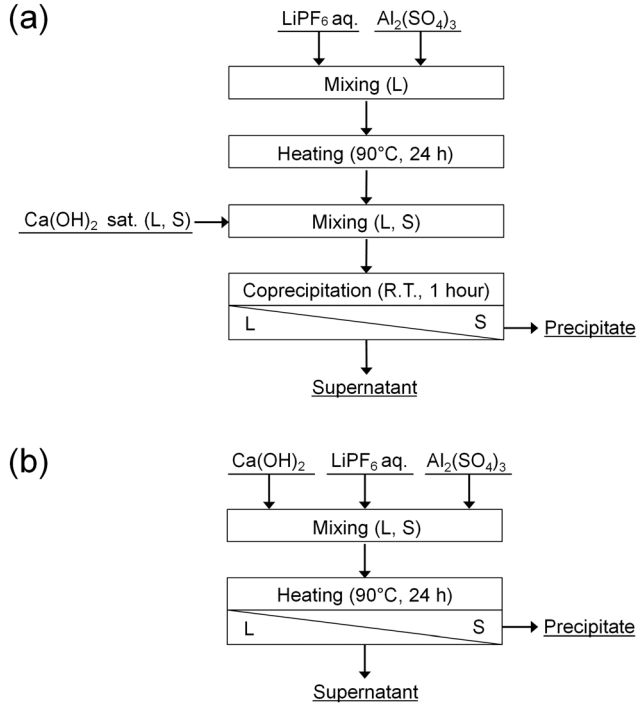

Fig. 1 Procedures (a) A and (b) B for the decomposition of PF_6^- and chemical precipitation of PO_4^{3-} and F^-.

solution (Nacalai Tesque, Inc., GR, 35%) to examine the effect of pH. Also, a sample solution containing 10 mM $LiPF_6$ and 100 mM $Al(NO_3)_3$ was prepared by using $Al(NO_3)_3{\cdot}9H_2O$ (Fujifilm Wako Pure Chemical Corporation, GR) to examine the effect of anions. The prepared sample solutions were placed in polypropylene (PP) screw containers with lids and were kept at R.T. or 90 °C for 24 h in a water bath (As One Corporation, HWA-50A). The concentrations of F^- and the pH were then measured after cooling to R.T. The decomposition percentage of PF_6^- was evaluated by quantifying the concentration of F^-, because F^- was produced as the decomposition of PF_6^- proceeds according to reaction (4).

Chemical precipitation after decomposition of PF_6^- by Al^{3+} in procedure A. The saturated $Ca(OH)_2$ slurry was prepared by adding $Ca(OH)_2$ powder (Nacalai Tesque, Inc., GR) more than its solubility (0.16 g/100 g H_2O, 21.6 mM at 298 K) into DI water. After the sample solution containing 10 mM $LiPF_6$ and 100 Al mM $Al_2(SO_4)_3$ was kept at 90 °C for 24 h, the saturated $Ca(OH)_2$ slurry was mixed with the sample solutions at a volume ratio of 1 : 1. The mixed solution was placed at R.T. for 1 h. Then, the supernatant and precipitate were separated by centrifugation, and the precipitate was dried under vacuum at R.T. The removal percentages of P and F were calculated according to eqn (5).

The pH and concentrations of the total P and total F in the supernatant were measured. The precipitate was subjected to phase identification by X-ray diffraction (XRD) and elemental analysis by wavelength dispersive spectroscopy (WDS).

Decomposition of PF_6^- and chemical precipitation in the aqueous solutions containing both $Al_2(SO_4)_3$ and $Ca(OH)_2$ at various prepared concentrations in procedure B. In procedure B, sample solutions containing 10 mM $LiPF_6$, 0–200 mM $Al_2(SO_4)_3$, and 108 mM $Ca(OH)_2$ were prepared by dissolving each reagent in DI water. These sample solutions were then kept at 90 °C for 24 h. The formation of precipitates was observed in each sample. In addition to the same analysis of the supernatant and precipitate as procedure A, quantification of the concentration of each anion was conducted.

2.2. Analysis

Measurement of pH using a pH electrode. The pH was measured using a pH electrode (Horiba, Ltd., 9632-10D), which was calibrated with standard solutions (pH 4.01, 6.86, and 9.18) according to the National Institute of Standard and Technology (NIST) standard methods. The pH measurements of the heated samples were performed after cooling to R.T.

Measurement of the F^- concentration using a fluoride-ion selective electrode. The F^-concentration in each sample solution was measured using a fluoride-ion selective electrode (Horiba, Ltd., 6561S-10C). Calibration was performed with 1 and 10 ppm or 10 and 100 ppm F^- standard solutions prepared using a 1000 ppm F^- standard solution (Fujifilm Wako Pure Chemical Corporation, Japan Calibration Service System (JCSS)). Before the measurements with the fluoride-ion selective electrode, the sample solutions were mixed with a total ionic strength adjustment buffer (TISAB) solution in a 1 : 1 volume ratio. Two types of TISAB solutions were prepared following American Society for Testing and Materials (ASTM) D1179 method B. TISAB 1 was prepared by dissolving 57 mL acetic acid (Nacalai Tesque, Inc., GR), 58 g NaCl (Nacalai Tesque, Inc., GR), and 0.3 g trisodium citrate dihydrate (Kanto Chemical Co., Inc., GR) in DI water to a volume of 1 L, and used for the sample solutions without Al^{3+}. TISAB 2 was prepared by dissolving 84 mL HCl solution, 242 g tris(hydroxymethyl)aminomethane (Nacalai Tesque, Inc., GR), and 230 g sodium (+)-tartrate dihydrate (Fujifilm Wako Pure Chemical Corporation., GR) in DI water to a volume of 1 L, and used for the sample solutions containing Al^{3+} to mitigate the interfering effect of Al^{3+}. As a preliminary test, sample solutions dissolving $Al_2(SO_4)_3$ and NaF were mixed with TISAB 1 or 2 solution and measured with a fluoride-ion selective electrode (Table S1†).

$$[\text{removal percentages}](\%) = \left(1 - \frac{[\text{amount of substance of P or F in supernatant}]\ (\text{mol})}{[\text{amount of substance of P or F in prepared solution}]\ (\text{mol})}\right) \times 100 \quad (5)$$

The results showed that the interfering effect of Al^{3+} was almost negligible in TISAB 2 when the Al^{3+} concentration was below 10 mM. Therefore, the sample solutions were diluted with DI water before the measurements so that the concentration of Al^{3+} was less than 10 mM.

Measurement of the total F concentration by the distillation method. For the determination of the total F concentration in the sample solutions, distillation was performed according to Japanese Industrial Standard (JIS) K 0102 for the quantification of the total F in various fluorine compounds. 1.0 mL of the sample solution, 0.2 g SiO_2 powder (Fujifilm Wako Pure Chemical Corporation., GR), 0.2 mL phosphoric acid (Nacalai Tesque, Inc., GR, 85%), 8 mL perchloric acid (Nacalai Tesque, Inc., GR, 60%), about 8 mL DI water, and some boiling stones were placed in a distillation flask. The temperature of the distillation flask was controlled at 145 ± 5 °C with steam blowing. The distillate was collected up to approximately 50 mL through a Liebig cooling pipe with cooling water. After adding DI water to the collected distillate to a volume of 100 mL, the F^- concentration was analyzed using the fluoride-ion selective electrode. The measured value may be lower than the true concentration because it depends on the recovery percentage of distillation.

Measurement of the total P and total Al concentrations by ICP-AES. Concentrations of the total P and total Al in sample solutions were determined by inductively coupled plasma atomic emission spectroscopy (ICP-AES, Hitachi High-Tech Science Corporation, SPS3520UV). The wavelengths used for the P and Al measurements were 177.496 nm and 237.312 nm, respectively. Standard solutions were prepared by diluting a standard solution of 1000 ppm P (Fujifilm Wako Pure Chemical Corporation., for water analysis) and 1000 ppm Al (Nacalai Tesque, Inc., SP) with 1 M HCl solution. The calibration curves were measured at four points respectively with the concentrations of 0 (blank), 10, 30, and 50 ppm P, and 0 (blank), 5, 10, and 20 ppm Al. Sample solutions were diluted with 1 M HCl solution to fit within the calibration range of the aimed elements. The average of two times measured values was used for the results.

Measurement of concentration of anions (PF_6^-, F^-, PO_4^{3-}, $PO_2F_2^-$) by ion chromatography. The quantification of anions in solution was performed by suppressed ion chromatography (Shimadzu Corporation, HIC-ESP) with a column (Shimadzu Corporation, Shim-pack IC-SA2), a suppressor (Shimadzu Corporation, ICDS-40A), and an electrical conductivity detector (Shimadzu Corporation, CDD-10AVP). A guard column (Shimadzu Corporation, Shim-pack IC-SA2(G)) and line filter (Shimadzu Corporation, A-356) were attached upstream of the analytical column. Column temperature was kept at 50 °C. The eluent was prepared by dissolving 3.6 mM Na_2CO_3 (Fujifilm Wako Pure Chemical Corporation., GR) and 3.4 mM $NaHCO_3$ (Fujifilm Wako Pure Chemical Corporation., GR) in DI water and flowed at a flow rate of 1.0 mL min^{-1}. The sample solutions to be measured were diluted one hundredfold with the eluent, and 20 μL of diluted solution was injected using a manual injector. The anions that could be formed during the decomposition of PF_6^- are F^-, PO_4^{3-}, $PO_2F_2^-$, and PO_3F^{2-}, and their concentrations were measured. The calibration curves were measured at three or more concentrations for each anion using standard sample solutions prepared using $LiPF_6$, $LiPO_2F_2$ (Tokyo Chemical Industry Co., Ltd., >98.0%), and Na_2PO_3F (Thermo Fisher Scientific K.K.), 1000 ppm PO_4^{3-} standard solution (Fujifilm Wako Pure Chemical Corporation, JCSS), 1000 ppm F^- standard solution, and 1000 ppm SO_4^{2-} standard solution (Fujifilm Wako Pure Chemical Corporation, JCSS). The ion chromatograms of the respective standard solutions used in this study are shown in Fig. S1.† In this study, PO_3F^{2-} could not be quantified for sample solutions containing SO_4^{2-} because their peaks overlap each other. The noise level was calculated by the average of the difference between the maximum and minimum values, accounting for drift, in each 0.5 min section without any peaks following the ASTM standards. The signal/noise (S/N) ratios of 3.3 and 10 were set as the detection limit and the limit of quantification, respectively.

Phase identification of precipitates by XRD and elemental analysis by WDS. An X-ray diffractometer (XRD, PANalytical, X'pert Pro, Cu-Kα line, 45 kV, 40 mA, θ–2θ method) was used for the phase identification of the precipitates. For the elemental analysis of the precipitates, wavelength dispersive spectroscopy (WDS, 15 kV, 50 nA, ZAF method) was performed with a field emission-electron probe micro analyzer (FE-EPMA, JEOL Ltd., JXA-8530F). Powdered samples were fixed on carbon tape, and carbon-coated with a carbon coater (Meiwafosis Co., Ltd., CADE-E) to give conductivity. In the mapping analysis, spot measurements were carried out at 0.5 μm × 0.5 μm intervals for a 60 μm × 43 μm area.

3. Results

3.1. Decomposition of PF_6^- in aqueous solution under various conditions

The F^- concentration indicates the decomposition progress of PF_6^-. The measured concentrations of F^- and pH are shown in Fig. 2, where 60 mM F^- corresponds to the complete decomposition reaction of 10 mM $LiPF_6$. The F^- concentration in each sample kept at R.T. is only less than 2 mM, but 54–56 mM F^- are detected for sample solutions kept at 90 °C in HCl solution with pH 1, 100 mM $Al_2(SO_4)_3$ solution, and 100 mM $Al(NO_3)_3$ solution. On the other hand, about 10 mM F^- is detected in HCl solution with pH 3, which is approximately equal to the pH in 100 mM $Al_2(SO_4)_3$ or 100 mM $Al(NO_3)_3$ solution before keeping. These results suggest that not only H^+ but also Al^{3+} accelerate the decomposition of PF_6^- at elevated temperatures. In $Al_2(SO_4)_3$ and $Al(NO_3)_3$ solutions, pH changes from around 3 to 1 are observed due to the formation of H^+ according to reaction (4).

3.2. Removal of P and F by adding $Ca(OH)_2$ after decomposition of PF_6^- by Al^{3+} (procedure A)

According to procedure A, the removal of P and F was examined by adding the saturated $Ca(OH)_2$ slurry after the decomposition of PF_6^- in $Al_2(SO_4)_3$ solution at 90 °C for 24 h.

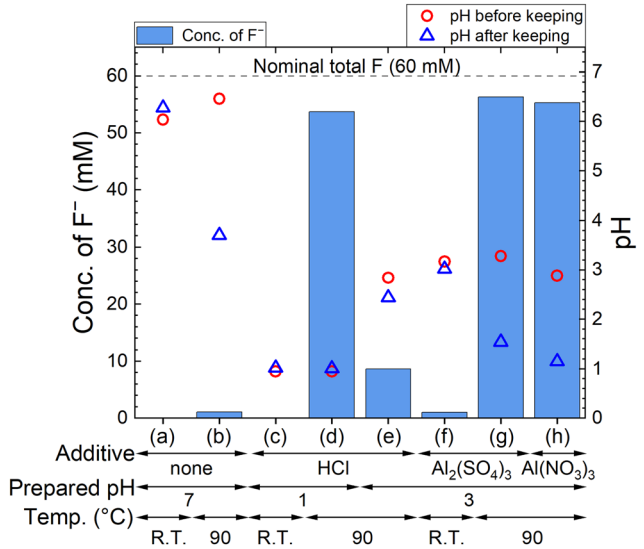

Fig. 2 Measured concentrations of F^- after keeping 10 mM $LiPF_6$ + none, HCl, $Al_2(SO_4)_3$, or $Al(NO_3)_3$ solution at R.T. or 90 °C for 24 h, and pH before and after keeping. The additive, prepared pH, and temperature are (a) none, 7, and R.T., (b) none, 7, and 90 °C, (c) HCl, 1, and R.T., (d) HCl, 1, and 90 °C, (e) HCl, 3, and 90 °C, (f) 100 mM $Al_2(SO_4)_3$, 3, and R.T., (g) 100 mM $Al_2(SO_4)_3$, 3, and 90 °C, and (h) 100 mM $Al(NO_3)_3$, 3, and 90 °C, respectively.

The removal percentages of P and F at 1 h after adding $Ca(OH)_2$ are shown in Fig. 3. In Exp. #01, the pH after adding 150 mM of $Ca(OH)_2$ is 4.3, and the removal percentages are 99% for P and 57% for F. On the other hand, the pH after adding 400 mM of $Ca(OH)_2$ is 10.6 in Exp. #02, and the removal percentages reach higher than 97% both for P and F. The removal percentages of P and F are enough or close to achieve the Japanese industrial effluent standards; the standards of 16 ppm and 8 ppm correspond to 0.516 mM for P and 0.421 mM for F, respectively.

The XRD pattern of the precipitate obtained in Exp. #02 is shown in Fig. 4. Strong peaks of $Ca_6Al_2(SO_4)_3(OH)_{12}{\cdot}26H_2O$ (ettringite) and weak peaks of $Ca(OH)_2$ are identified. The formation of ettringite is expected according to reaction (6).

$$Al_2(SO_4)_3 + 6Ca(OH)_2 \rightarrow Ca_6Al_2(SO_4)_3(OH)_{12} \quad (6)$$

To evaluate the formation of a compound containing P or F, the precipitate was analyzed by FE-EPMA and WDS. The obtained scanning electron microscope (SEM) image and elemental distribution mappings are shown in Fig. 5. Sulfur, Ca, and Al coexist in the same grains, and they are expected to be ettringite. P and F are also observed in the ettringite, and PO_4^{3-} and F^- are suggested to be coprecipitated with ettringite.

3.3. Removal of P and F *via* decomposition of PF_6^- in $Al_2(SO_4)_3$ + $Ca(OH)_2$ solutions (procedure B)

According to procedure B, the decomposition of PF_6^- and the removal percentages of P and F were examined in $Ca(OH)_2$ + $Al_2(SO_4)_3$ solutions. The removal percentages of P and F in the supernatant kept at 90 °C for 24 h are shown in Fig. 6(a) and the pH levels before and after keeping are shown in Fig. 6(b). The removal percentage of P significantly increases when the $Al_2(SO_4)_3$ concentration is higher than 70 mM and reaches 85–98% at 100 mM. The removal percentage of F also shows a similar trend, reaching about 40% at 100 mM. As shown in Fig. 6(b), the pH decreases from about 4 to 2.5–3.5 before and after keeping for 24 h at 100 mM. For the representative conditions, the concentrations of the

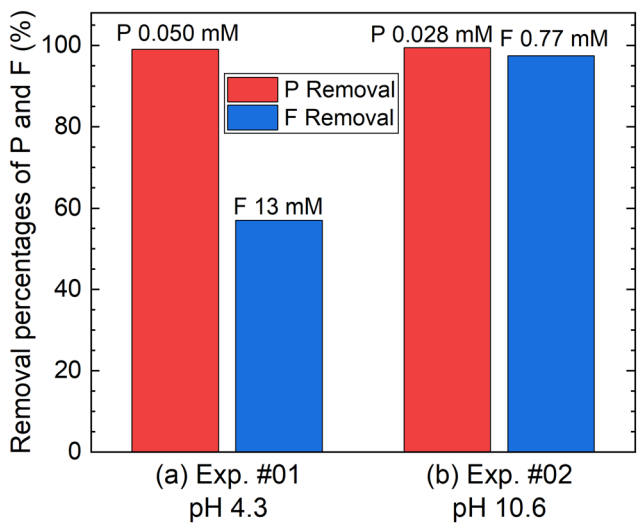

Fig. 3 Removal percentages of P and F after keeping the 10 mM $LiPF_6$ + 100 Al mM $Al_2(SO_4)_3$ solution at 90 °C for 24 h following the addition of (a) 150 mM or (b) 400 mM of saturated $Ca(OH)_2$ slurry at a volume ratio of 1 : 1 according to procedure A. The numbers above the bar graph indicate the measured concentrations of the supernatant of the total P or total F.

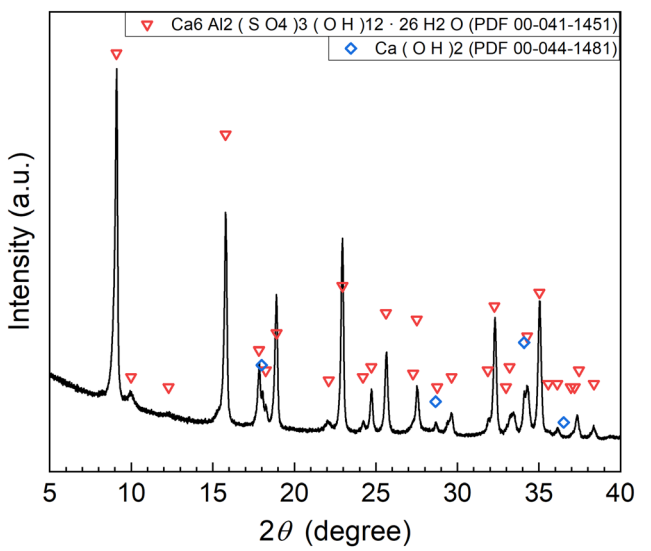

Fig. 4 XRD pattern of the precipitate obtained after keeping the 10 mM $LiPF_6$ + 100 Al mM $Al_2(SO_4)_3$ solution at 90 °C for 24 h following the addition of 400 mM $Ca(OH)_2$ as the saturated slurry (Exp. #02) according to procedure A.

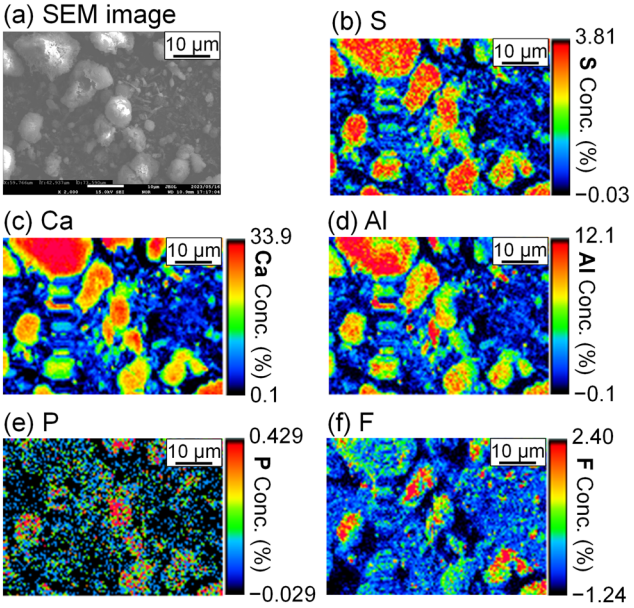

Fig. 5 (a) SEM image and WDS mappings for (b) S, (c) Ca, (d) Al, (e) P, and (f) F of the precipitate obtained after keeping the 10 mM $LiPF_6$ + 100 Al mM $Al_2(SO_4)_3$ solution at 90 °C for 24 h following the addition of 400 mM of saturated $Ca(OH)_2$ slurry (Exp. #02) according to procedure A.

respective anions are shown in Table 1 and the ion chromatograms are shown in Fig. S2.† The precipitates were formed under all conditions. The difference of the total P concentrations calculated from the sum of species by chromatography with those measured by other methods is not significantly high, and the same can be correct for the total F concentrations. Other chemical species containing P or F which are not listed in Table 1 are expected to be therefore almost absent. When the prepared concentration of $Al_2(SO_4)_3$ is 0 or 50 mM (Exp. #03 and #04), the concentration of PF_6^- in the supernatant after keeping is 9.6 or 9.0 mM, and only small amounts of other anions containing P or F are detected. On the other hand, at 100–150 mM (Exp. #05 and #06), PF_6^- is not detected but PO_4^{3-} and F^- are significantly detected with a large decrease in the total P and total F concentrations. In procedure B, Exp. #03 and #04 suggest that PF_6^- is stable at 0–50 mM, and Exp. #05 and #06 demonstrate that PF_6^- is decomposed and P and F are precipitated. It is noted that there is no significant pH decrease as observed in procedure A.

The XRD patterns of the obtained precipitates are shown in Fig. 7. Depending on the added amount of $Al_2(SO_4)_3$, $Ca(OH)_2$, ettringite, and/or $CaSO_4{\cdot}2H_2O$ (gypsum) are identified. The formation of ettringite and gypsum is expected according to reactions (6) and (7), respectively.

$$Al_2(SO_4)_3 + 3Ca(OH)_2 \rightarrow 3CaSO_4 + 2Al(OH)_3 \quad (7)$$

The stoichiometric molar ratios of Al/Ca in reactions (6) and (7) are 1/3 and 2/3, respectively, and the compounds in the precipitate are expected to depend on the molar ratio of

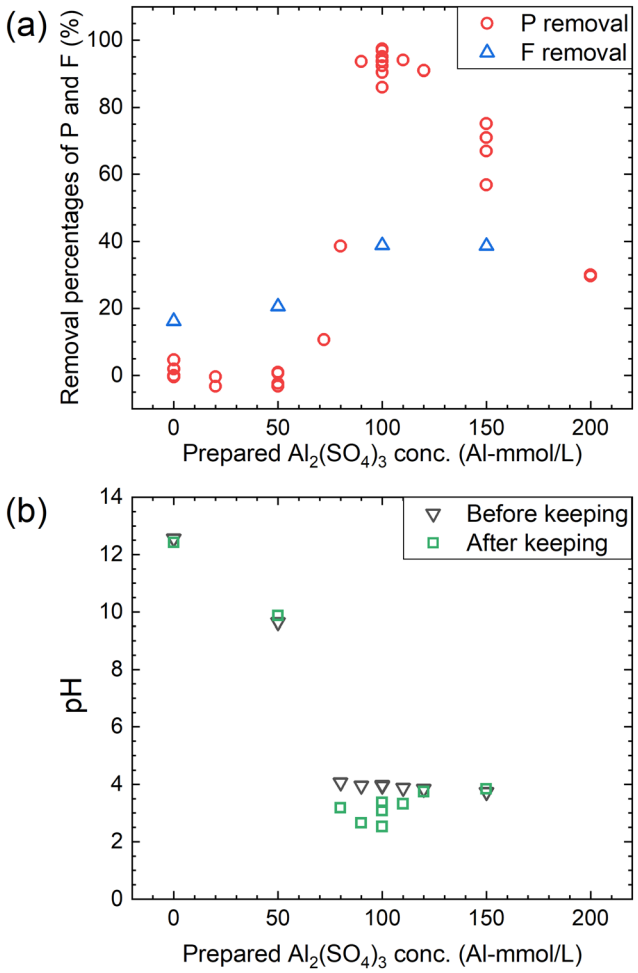

Fig. 6 (a) Removal percentages of P and F after keeping the 10 mM $LiPF_6$ + 0–200 Al mM $Al_2(SO_4)_3$ + 108 mM $Ca(OH)_2$ solutions at 90 °C for 24 h according to procedure B and (b) the pH before and after keeping.

Al/Ca at the prepared concentrations. In view of this, ettringite and excess $Ca(OH)_2$ are expected to be in the precipitate for Al/Ca < 1/3, ettringite, gypsum, and $Al(OH)_3$ for 1/3 < Al/Ca < 2/3, and gypsum and $Al(OH)_3$ for Al/Ca > 2/3. In Fig. 7, ettringite and $Ca(OH)_2$ are detected by XRD for Al/Ca = 0.19 (Exp. #07), ettringite and gypsum for Al/Ca = 0.46 (Exp. #04), and only gypsum for Al/Ca = 0.93 (Exp. #05) and 1.4 (Exp. #06); the compounds are detected as expected from the stoichiometric ratios of Al/Ca in reactions (6) and (7) except for $Al(OH)_3$. In procedure B, the removal percentages of P and F are maximum (86% for P and 38% for F) when Al/Ca = 0.93 (Exp. #05). To evaluate the formation of a compound containing P and F, SEM and WDS were conducted for the precipitate obtained in Exp. #05 and the results are shown in Fig. 8. Only gypsum is detected by XRD, and the grains where S and Ca coexist are expected to be gypsum. The Al grains independently distributed are also observed and may be $Al(OH)_3$ in amorphous form. Here, P and F are observed in the amorphous $Al(OH)_3$, suggesting that PO_4^{3-} and F^- are coprecipitated with amorphous $Al(OH)_3$.

Table 1 Results of measurements of the supernatant obtained in procedure B

Exp. #	Prepared concentration			Measured concentration (mM)								Removal rate (%)		pH	
				Ion chromatography[a]						ICP[b]	Distillation[c]	ICP	Distillation		
	$LiPF_6$ (mM)	$Ca(OH)_2$ (mM)	$Al_2(SO_4)_3$ (Al mM)	PF_6^-	F^-	PO_4^{3-}	$PO_2F_2^-$	Total P	Total F	Total P	Total F	P	F	Before	After
03	10	108	0	9.6	0.42	n.d.[d]	<0.057[e]	9.6	58	10	50	0.0	17	12.6	12.5
04	10	108	50	9.0	{0.19}[f]	<0.13[e]	n.d.[d]	9.0	54	9.9	48	1.0	20	9.6	10.2
05	10	108	100	n.d.[d]	43	0.58	n.d.[d]	0.58	43	1.4	37	86	38	4.0	2.7
06	10	108	150	n.d.[d]	51	2.4	{0.087}[f]	2.4	51	2.9	37	71	38	3.8	3.8

[a] Measured by ion chromatography. [b] Measured by ICP-AES. [c] Measured by the distillation method. [d] Below the detection limit. [e] Below the limit of quantification. [f] {} means "out of the concentration range in the calibration curve".

The measured concentrations of the total Al in the supernatants of each sample kept at 90 °C for 24 h according to procedure B are shown in Fig. 9. The total Al concentration is below the detection limit at Al/Ca < 2/3, but it increases at Al/Ca > 2/3. Excess Al^{3+} for reaction (7) is present in the supernatant when Al/Ca is greater than the stoichiometric molar ratio in reaction (7), 2/3, and the decomposition of PF_6^- is expected to proceed due to the excess Al^{3+} (Exp. #05 and #06).

4. Discussion

4.1. Comparison of procedures A and B

The features of the reactions in procedures A and B are schematically illustrated in Fig. 10. The progress of the decomposition of PF_6^- and the coprecipitation with PO_4^{3-} and F^- depends on the molar ratio of Al/Ca at the prepared concentration of $Ca(OH)_2$ and $Al_2(SO_4)_3$. The decomposition of PF_6^- is accelerated by Al^{3+} where Ca = 0 (procedure A) or Al/Ca is greater than 2/3 (procedure B). In procedure A, Exp. #02 showed that the addition of $Ca(OH)_2$ at the molar ratio of Al/Ca = 0.25 leads to the precipitation removal of PO_4^{3-} and F^-. The molar ratio of Al/Ca = 0.25 corresponds to the area of Al/Ca < 1/3, where ettringite is formed with excess $Ca(OH)_2$ at pH 12. In procedure B, some PO_4^{3-} and F^- produced by the decomposition are coprecipitated with $Al(OH)_3$ at Al/Ca > 2/3 without additional $Ca(OH)_2$.

Here, Exp. #02 showed that the removal percentages of P and F were higher than 97% in procedure A, but in procedure B, Exp. #05 showed that the removal percentages were only 86% for P and 38% for F. It is noted that the molar ratios of Al/Ca in Exp. #02 and #05 are 0.25 and 0.93, respectively. Experimental results show that the removal percentages of P

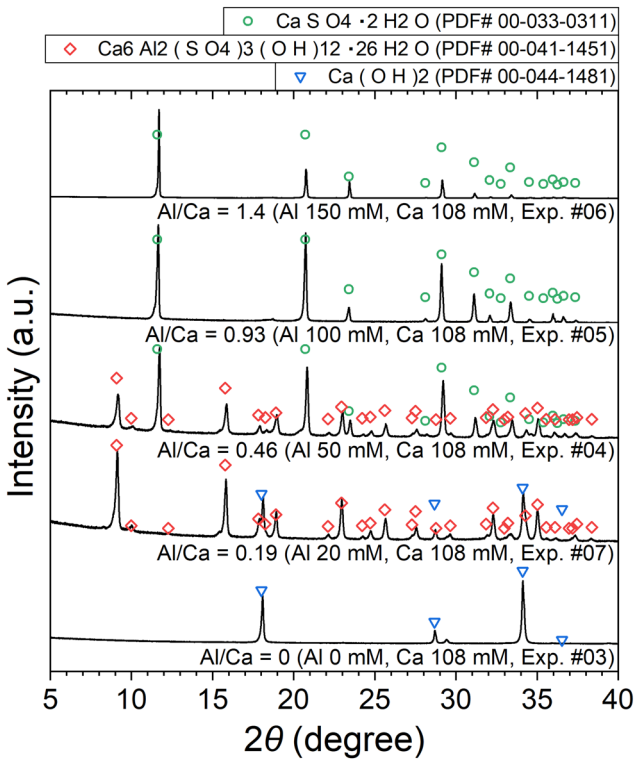

Fig. 7 XRD patterns of the precipitates obtained after keeping the 10 mM $LiPF_6$ + 0–150 Al mM $Al_2(SO_4)_3$ + 108 mM $Ca(OH)_2$ solutions at 90 °C for 24 h (Exp. #03–07) according to procedure B.

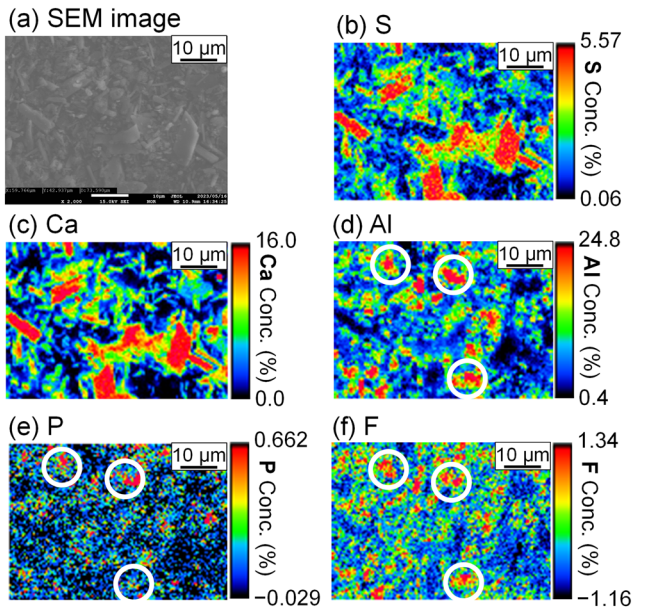

Fig. 8 (a) SEM image and WDS mappings for (b) S, (c) Ca, (d) Al, (e) P, and (f) F of the precipitate obtained after keeping the 10 mM $LiPF_6$ + 100 Al mM $Al_2(SO_4)_3$ + 108 mM $Ca(OH)_2$ solution at 90 °C for 24 h (Exp. #05) according to procedure B. The white circles are representative grains where Al, P, and F coexist.

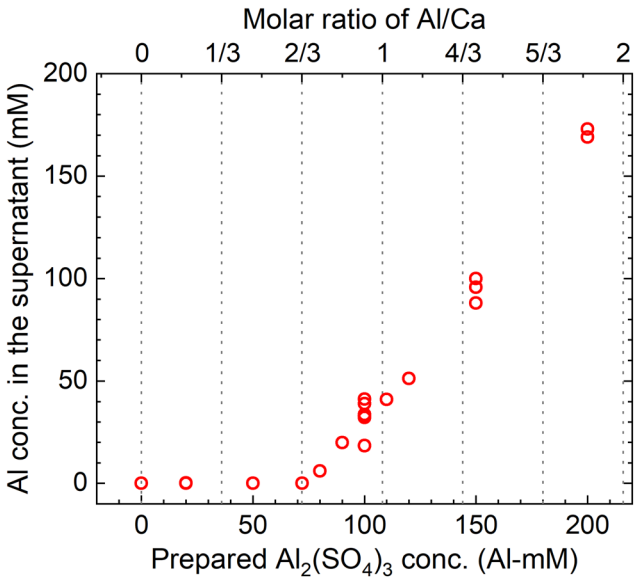

Fig. 9 Measured concentrations of the total Al in the supernatant after keeping the 10 mM $LiPF_6$ + 0–200 Al mM $Al_2(SO_4)_3$ + 108 mM $Ca(OH)_2$ solutions at 90 °C for 24 h according to procedure B.

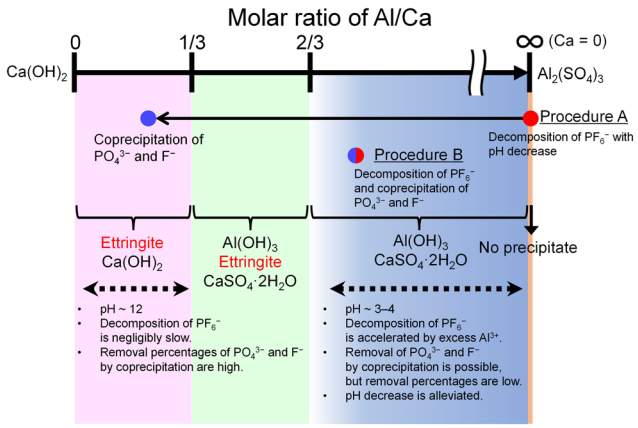

Fig. 10 Schematic illustration of the features of the reactions in procedures A and B.

and F are expected to depend on the molar ratio of Al/Ca. Higher removal percentages of P and F are achieved by adding sufficient $Ca(OH)_2$ after finishing the decomposition in procedure B so that the molar ratio of Al/Ca shifts from Al/Ca > 2/3 to Al/Ca < 1/3, as well as in procedure A.

It is better for practical operation at high temperature to avoid strong acid conditions such as pH = 1 or less, but the pH decreases due to H^+ produced during the decomposition of PF_6^-. For the decomposition of 1 mol PF_6^-, 8 mol H^+ is produced according to reaction (4). The experimental results in procedure A show that the pH decrease in the decomposition of 10 mM PF_6^- with 100 mM Al^{3+} was approximately from 3 to 1 as shown in Fig. 2. In procedure B, on the other hand, the pH decrease accompanying the decomposition is alleviated; for example, the pH decrease in the decomposition of 10 mM PF_6^- in 100 mM $Al_2(SO_4)_3$ + 108 mM $Ca(OH)_2$ is only from 4.0 to 2.7 in Table 1. The smaller pH decrease is attributed to $Al(OH)_3$ formed according to reaction (7). The $Al(OH)_3$ precipitate reacts with H^+ produced during the decomposition, acting as a buffer to alleviate the pH decrease according to reaction (8).[31]

$$Al(OH)_3 + 3H^+ \rightleftarrows Al^{3+} + 3H_2O \quad \text{Log}\,K = 8.291 \qquad (8)$$

4.2. Precipitation mechanism of PO_4^{3-} and F^-

The simultaneous chemical precipitation of PO_4^{3-} and F^- was reported in several past studies, and the formed precipitates were $Ca_5(PO_4)_3OH$ (hydroxylapatite) and/or CaF_2 (fluorite).[32,33] However, PO_4^{3-} and F^- were coprecipitated with ettringite and/or $Al(OH)_3$, and the formation of hydroxylapatite and fluorite was not observed in this study. To clarify the precipitation mechanism of PO_4^{3-} and F^-, the results in this study were also discussed from the view of thermodynamic equilibrium. The equilibrium of dissolving chemical species and precipitation was calculated on PHREEQC version 2 released by the U.S. Geological Survey.[34] The precipitates subjected to the calculation are ettringite, gypsum, hydroxylapatite, fluorite, gibbsite, and $Ca(OH)_2$, and the adopted equilibrium constants are shown in Table 2. The equilibrium constant in the PHREEQC database, minteq.v4.dat.,[31] was used. Only for the dissolution equilibrium constant of ettringite, the value reported by Perkins *et al.*[35] was adopted. In this study, $Al(OH)_3$ was formed as an amorphous form, but the equilibrium constant of gibbsite, the most stable species in the database, was used in the calculation. The definition of PF_6^- is not given in minteq.v4.dat., and it is newly defined as a monovalent anion that does not react with other chemical species. The input concentrations are shown in Table 3. Condition A shown in Table 3 corresponds to procedure A shown in Fig. 1(a), in which a solution containing $Al_2(SO_4)_3$ and totally decomposed $LiPF_6$ is mixed with $Ca(OH)_2$ solution at each concentration. Condition B corresponds to procedure B shown in Fig. 1(b), *i.e.*, a solution containing a fixed amount of $LiPF_6$ and $Ca(OH)_2$, and

Table 2 Precipitation species and their equilibrium constants at 297 K adopted for the equilibrium calculation

Precipitate names	Formula	Reactions	Log *K*	Ref.
Ettringite	$Ca_6Al_2(OH)_{12}(SO_4)_3{\cdot}26H_2O$	$Ca_6Al_2(OH)_{12}(SO_4)_3{\cdot}26H_2O = 6Ca^{2+} + 2Al(OH)_4^- + 3SO_4^{2-} + 4OH^- + 26H_2O$	−44.9	Perkins *et al.*[35]
Gypsum	$CaSO_4{\cdot}2H_2O$	$CaSO_4{\cdot}2H_2O = Ca^{2+} + SO_4^{2-} + 2H_2O$	−4.61	minteq.v4.dat[31]
Hydroxylapatite	$Ca_5(PO_4)_3OH$	$Ca_5(PO_4)_3OH + H^+ = 5Ca^{2+} + 3PO_4^{3-} + H_2O$	−44.333	minteq.v4.dat
Fluorite	CaF_2	$CaF_2 = Ca^{2+} + 2F^-$	−10.5	minteq.v4.dat
Gibbsite	$Al(OH)_3$	$Al(OH)_3 + 3H^+ = Al^{3+} + 3H_2O$	8.291	minteq.v4.dat
Portlandite	$Ca(OH)_2$	$Ca(OH)_2 + 2H^+ = Ca^{2+} + 2H_2O$	22.804	minteq.v4.dat

Table 3 Input value of concentrations of chemical species adopted for the equilibrium calculation

Chemical species	Input value of concentrations	
	Condition A	Condition B
$Ca(OH)_2$	From 0 mM to 250 mM in 500 steps	108 mM
$Al_2(SO_4)_3$	50 Al mM	From 0 Al mM to 200 Al mM in 500 steps
Li^+	5 mM	10 mM
PF_6^-	0 mM	10 mM for Al/Ca < 2/3 0 mM for Al/Ca > 2/3
PO_4^{3-}	5 mM	0 mM for Al/Ca < 2/3 10 mM for Al/Ca > 2/3
F^-	30 mM	0 mM for Al/Ca < 2/3 60 mM for Al/Ca > 2/3

$Al_2(SO_4)_3$ at each concentration. As a simplified condition of the experimental results of this study, condition B used here is that PF_6^- is not decomposed at all for Al/Ca < 2/3 and is decomposed completely for Al/Ca > 2/3. The full text of the input data is summarized in the ESI.†

The molar amounts of precipitates equilibrated for each concentration are shown in Fig. 11. The graphs shown in Fig. 11(a) and (b) show the results for conditions A and B, respectively. Under condition A, gypsum, gibbsite, and hydroxylapatite are formed corresponding to Exp. #01, and ettringite, fluorite, $Ca(OH)_2$, and hydroxylapatite to Exp. #02, as shown in Fig. 11(a). On the other hand, the experimental results indicated that neither fluorite nor hydroxylapatite was observed by the analysis of XRD (Fig. 4), and WDS (Fig. 5) analysis showed that P and F are coprecipitated with ettringite. The difference between the calculation and experiment results is possibly due to the ion exchange ability of ettringite. The ion exchange behavior of SO_4^{2-} in ettringite with other anions in aqueous solutions such as PO_4^{3-} or F^- was reported.[36,37] The ion exchange reaction may be superior in terms of thermodynamics or kinetics to the formation of fluorite and/or hydroxylapatite.

Under condition B, $Ca(OH)_2$ is formed corresponding to Exp. #03, ettringite and $Ca(OH)_2$ to Exp. #07, gypsum, gibbsite, and ettringite to Exp. #04, and gypsum and gibbsite to Exp. #05 and 06, as shown in Fig. 11(b). These results are consistent with the experimental results in section 3.3, except for the coprecipitation of PO_4^{3-} and F^- with $Al(OH)_3$. The coprecipitation of PO_4^{3-} and F^- in this study was expected to proceed by surface adsorption on formed $Al(OH)_3$, as these anions are reported to precipitate by surface adsorption on $Al(OH)_3$.[38–40]

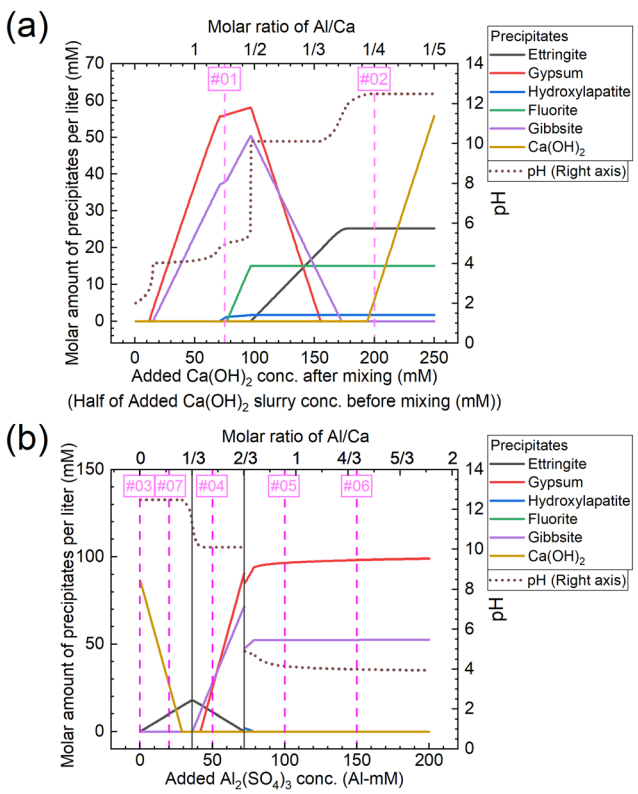

Fig. 11 Molar amounts of precipitates equilibrated for each concentration of (a) added $Ca(OH)_2$ under condition A and (b) added $Al_2(SO_4)_3$ under condition B shown in Table 3. The numbers #0*x* (*x* = 1–7) in the graph correspond to the same conditions as Exp. #0*x*.

5. Conclusion

In this study, the decomposition of PF_6^- in aqueous solution was demonstrated to be accelerated when Al^{3+} was contained in the solution at an elevated temperature. The decomposition of PF_6^- is negligibly slow when the solution contained no additive or the solution temperature was room temperature, but it was accelerated when the solution at pH 1 or containing 100 mM Al^{3+} at pH 3 was kept at 90 °C for 24 h. In procedure A, after PF_6^- was decomposed by Al^{3+}, the produced PO_4^{3-} and F^- were removed from the precipitate by adding sufficient $Ca(OH)_2$ and the removal percentages of P and F were higher than 97%. The precipitate was ettringite, and PO_4^{3-} and F^- were coprecipitated with it. The decomposition of PF_6^- was accompanied by a pH decrease due to the formation of H^+. In procedure B, PF_6^- was decomposed in pre-mixed solutions of $Al_2(SO_4)_3$ and $Ca(OH)_2$ at the prepared molar ratio of Al/Ca > 2/3, and the pH decrease during the decomposition of PF_6^- was alleviated. The alleviation of the pH decrease is expected to be due to the buffer effect of the $Al(OH)_3$ precipitate formed by the reaction of $Al_2(SO_4)_3$ and $Ca(OH)_2$. The produced PO_4^{3-} and F^- were coprecipitated with $Al(OH)_3$, but the removal percentages were only 86% for P and 38% for F. For higher removal percentages of P and F, the addition of sufficient $Ca(OH)_2$ is expected to be required after the decomposition.

Author contributions

All authors conceived the ideas. T. M. contributed to the execution of the experiments, wrote the manuscript, and performed the analysis. All authors reviewed the manuscript.

Conflicts of interest

There are no conflicts to declare.

Acknowledgements

This work was financially supported by the Adaptable and Seamless Technology transfer Program through Target-driven R&D (A-STEP), Grant Number JPMJTR20TF from Japan Science and Technology Agency (JST), and the establishment of university fellowships towards the creation of science technology innovation, Grant Number JPMJFS2123 from JST. This work was conducted as a collaboration research of the Laboratory of Design of Sustainable Materials and Processing and the Laboratory of Non-ferrous Extractive Metallurgy, Department of Materials Science and Engineering, Graduate School of Engineering, Kyoto University. The Laboratory of Non-ferrous Extractive Metallurgy is an endowed chair by Mitsubishi Material Corp. We would like to acknowledge Dr. Akihiro Kishimoto, Dr. Takumi Yasuda at Kyoto University, and Prof. Takashi Nakamura at Tohoku University for fruitful discussion.

Notes and references

1 Y. Tao, Z. Wang, B. Wu, Y. Tang and S. Evans, Environmental life cycle assessment of recycling technologies for ternary lithium-ion batteries, *J. Cleaner Prod.*, 2023, **389**, 136008.
2 C. H. Illa Font, H. V. Siqueira, J. E. Machado Neto, J. L. F. D. Santos, S. L. Stevan, A. Converti and F. C. Corrêa, Second life of lithium-ion batteries of electric vehicles: A short review and perspectives, *Energies*, 2023, **16**, 953.
3 F. Maisel, C. Neef, F. Marscheider-Weidemann and N. F. Nissen, A forecast on future raw material demand and recycling potential of lithium-ion batteries in electric vehicles, *Resour., Conserv. Recycl.*, 2023, **192**, 106920.
4 J. Neumann, M. Petranikova, M. Meeus, J. D. Gamarra, R. Younesi, M. Winter and S. Nowak, Recycling of lithium-ion batteries—Current state of the art, circular economy, and next generation recycling, *Adv. Energy Mater.*, 2022, **12**, 2102917.
5 R. Sommerville, J. Shaw-Stewart, V. Goodship, N. Rowson and E. Kendrick, A review of physical processes used in the safe recycling of lithium ion batteries, *Sustainable Mater. Technol.*, 2020, **25**, e00197.
6 H. Pinegar and Y. R. Smith, Recycling of end-of-life lithium ion batteries, Part I: Commercial processes, *J. Sustain. Metall.*, 2019, **5**, 402–416.
7 D. Cheret and S. Santen, *US Pat.*, US7169206B2, 2007.
8 Y. Yamaguchi, *JP Pat.*, JP5657730B2, 2015.
9 M. Kudo and S. Shimizu, *JP Pat.*, JP3069306B2, 2000.
10 W. N. Smith and S. Swoffer, *US Pat.*, US8616475B1, 2013.
11 A. Kochhar and T. G. Johnston, *US Pat.*, US10919046B2, 2021.
12 F. Tedjar and J.-C. Foudraz, *US Pat.*, US7820317B2, 2010.
13 T. Uda, A. Kishimoto, K. Yasuda and Y. Taninouchi, Submerged comminution of lithium-ion batteries in water in inert atmosphere for safe recycling, *Energy Adv.*, 2022, **1**, 935–940.
14 T. Fujita, H. Chen, K. Wang, C. He, Y. Wang, G. Dodbiba and Y. Wei, Reduction, reuse and recycle of spent Li-ion batteries for automobiles: A review, *Int. J. Miner., Metall. Mater.*, 2021, **28**, 179–192.
15 E. Mossali, N. Picone, L. Gentilini, O. Rodrìguez, J. M. Pérez and M. Colledani, Lithium-ion batteries towards circular economy: A literature review of opportunities and issues of recycling treatments, *J. Environ. Manage.*, 2020, **264**, 110500.
16 J. T. Bunce, E. Ndam, I. D. Ofiteru, A. Moore and D. W. Graham, A review of phosphorus removal technologies and their applicability to small-scale domestic wastewater treatment systems, *Front. Environ. Sci.*, 2018, **6**, 8.
17 G. Morse, S. Brett, J. Guy and J. Lester, Review: Phosphorus removal and recovery technologies, *Sci. Total Environ.*, 1998, **212**, 69–81.
18 V. Khatibikamal, A. Torabian, F. Janpoor and G. Hoshyaripour, Fluoride removal from industrial wastewater using electrocoagulation and its adsorption kinetics, *J. Hazard. Mater.*, 2010, **179**, 276–280.
19 A. Bhatnagar, E. Kumar and M. Sillanpää, Fluoride removal from water by adsorption—A review, *Chem. Eng. J.*, 2011, **171**, 811–840.
20 C. F. Z. Lacson, M.-C. Lu and Y.-H. Huang, Fluoride-containing water: A global perspective and a pursuit to sustainable water defluoridation management – An overview, *J. Cleaner Prod.*, 2021, **280**, 124236.
21 K. Tasaki, K. Kanda, S. Nakamura and M. Ue, Decomposition of $LiPF_6$ and stability of PF_5 in Li-ion battery electrolytes. Density functional theory and molecular dynamics studies, *J. Electrochem. Soc.*, 2003, **150**, A1628–A1636.
22 M. Stich, M. Göttlinger, M. Kurniawan, U. Schmidt and A. Bund, Hydrolysis of $LiPF_6$ in carbonate-based electrolytes for lithium-ion batteries and in aqueous media, *J. Phys. Chem. C*, 2018, **122**, 8836–8842.
23 B. Emmanuel and L. Richard, *WO Pat.*, WO2016012941A1, 2016.
24 O. A. Zalat and M. A. Elsayed, A study on microwave removal of pyridine from wastewater, *J. Environ. Chem. Eng.*, 2013, **1**, 137–143.
25 K. Kim, I. Park, S.-Y. Ha, Y. Kim, M.-H. Woo, M.-H. Jeong, W. C. Shin, M. Ue, S. Y. Hong and N.-S. Choi, Understanding the thermal instability of fluoroethylene carbonate in $LiPF_6$-based electrolytes for lithium ion batteries, *Electrochim. Acta*, 2017, **225**, 358–368.
26 W. N. Smith and S. Swoffer, *WO Pat.*, WO2013054875, 2013.
27 H. Kikuyama, T. Fukutome and M. Miyashita, *US Pat.*, US6666973, 2003.
28 Y. Mochida, *JP Pat.*, JP1994170380, 1994.
29 J. Brosheer, F. Lenfesty and K. Elmore, Vapor Pressure of Hydrofluoric Acid Solutions, *Ind. Eng. Chem.*, 1947, **39**, 423–427.
30 H. R. Clark and M. M. Jones, Ligand substitution catalysis via hard acid-hard base interaction, *J. Am. Chem. Soc.*, 1970, **92**, 816–822.

31 D. Allison, D. S. Brown and K. J. Novo-Gradac, *MINTEQA2/PRODEFA2, a Geochemical assessment model for environmental systems: Version 3.0 user's manual*, Environmental Research Laboratory, Office of Research and Development, U.S. Environmental Protection Agency, US, 1991.

32 C. F. Z. Lacson, M.-C. Lu and Y.-H. Huang, Calcium-based seeded precipitation for simultaneous removal of fluoride and phosphate: Its optimization using BBD-RSM and defluoridation mechanism, *J. Water Proc.engineering*, 2022, **47**, 102658.

33 H.-J. Ho, M. Takahashi and A. Iizuka, Simultaneous removal of fluoride and phosphate from semiconductor wastewater via chemical precipitation of calcium fluoride and hydroxyapatite using byproduct of recycled aggregate, *Chemosphere*, 2023, **340**, 139875.

34 PHREEQCE Welcome page, **https://wwwbrr.cr.usgs.gov/projects/GWC_coupled/phreeqe/**, (accessed January 2024).

35 R. B. Perkins and C. D. Palmer, Solubility of ettringite ($Ca_6[Al(OH)_6]_2(SO_4)_3 \cdot 26H_2O$) at 5–75°C, *Geochim. Cosmochim. Acta*, 1999, **63**(13–14), 1969–1980.

36 Y. Kamimoto, K. Onda, R. I. Ichino, K.-S. Min, K.-H. Kwon and Y.-J. Jung, Removal properties of phosphate with Ettringite, *Desalin. Water Treat.*, 2017, 478–482.

37 A. Iizuka, H.-J. Ho and A. Yamasaki, Removal of fluoride ions from aqueous solution by metaettringite, *PLoS One*, 2022, **17**(3), e0265451.

38 W. H. Van Riemsdijk and J. Lyklema, Reaction of phosphate with gibbsite ($AI(OH)_3$) beyond the adsorption maximum, *J. Colloid Interface Sci.*, 1980, **76**(1), 55–66.

39 S. Gypser, F. Hirsch, A. M. Schleicher and D. Freese, Impact of crystalline and amorphous iron- and aluminum hydroxides on mechanisms of phosphate adsorption and desorption, *J. Environ. Sci.*, 2018, **70**, 175–189.

40 X. Liu, Y. Wang, X. Cui, S. Zhu and J. Cao, Fluoride removal from wastewater by natural and modified gibbsite, *J. Chem. Eng. Data*, 2021, **66**(1), 658–668.